Inorganica Chimica Acta, 179 (1991) 255–265

FT-IR study of surface species derived from $[(\eta\text{-}C_5H_5)Ru(CO)_2]_2$ on oxide supports

S. Dobos
Institute of Isotopes, Hungarian Academy of Sciences, P.O.B. 77, H-1525 Budapest (Hungary)

B. V. Lokshin
Institute of Organoelement Compounds, Academy of Sciences, Vavilova 28, 117813 Moscow (U.S.S.R.)

and **S. G. Kazarian**
Institute of Spectroscopy, Academy of Sciences, Troitzk, Moscow region (U.S.S.R.)

(Received May 21, 1990; revised September 4, 1990)

Abstract

Surface reactions of $[(\eta\text{-}C_5H_5)Ru(CO)_2]_2$ adsorbed on partly dehydroxylated alumina and silica surfaces at room temperature and thermal stability of surface species in the temperature range of 303–723 K have been followed by FT-IR spectroscopy. Model reactions of $[(\eta\text{-}C_5H_5)Ru(CO)_2]_2$ and, for comparison, those of $[(\eta\text{-}C_5H_5)Fe(CO)_2]_2$ in liquid xenon solutions have also been performed. As main surface species 1:1 and 1:2 hydrogen bonded complexes, 1:1 and 1:2 adducts with surface Lewis acid sites, $(\eta\text{-}C_5H_5)(CO)_2Ru\text{–}H^+\text{–}Ru(CO)_2(\eta\text{-}C_5H_5)$ protonated molecules, $[(\eta\text{-}C_5H_5)(CO)_2Ru\text{–}O\text{–}]$, $Ru^{(0,II)}(CO)_2$ (on alumina, only) monomeric surface anchored species were detected. The possibility of the existence of the $(\eta\text{-}C_5H_5)(CO)_2Ru\text{–}H^+\text{–}Ru(CO)_2(\eta\text{-}C_5H_5)$ molecule stabilized on the surface by coordination to surface O^- has been discussed on the base of results gained from model measurements in liquid xenon solutions.

Introduction

Recently we reported FT-IR studies of the interaction of the $[(\eta\text{-}C_5H_5)Fe(CO)_2]_2$ molecule with hydroxylated alumina and silica surfaces [1, 2]. As main products of surface reactions the very stable tetrameric $[(\eta\text{-}C_5H_5)Fe(\mu\text{-}CO)]_4$ and the less stable monomeric $[(\eta\text{-}C_5H_5)(CO)_2Fe\text{–}O\text{–}]$ species were detected on both supports. In addition, at room temperature in the very first steps of the cluster – support interaction, we simultaneously identified a whole series of different surface complexes of the $[(\eta\text{-}C_5H_5)Fe(CO)_2]_2$ molecule, like hydrogen bonded species of one or both bridging carbonyls with surface hydroxyls, adduct type complexes with surface Lewis acidic sites, and monomer cyclopentadienyl carbonyls, together with the original, unperturbed $[(\eta\text{-}C_5H_5)Fe(CO)_2]_2$. Protonation of the metal–metal bond was also supposed, although not confirmed.

In the case of $[(\eta\text{-}C_5H_5)Fe(CO)_2]_2$ the high number and the considerable stability of the surface complexes are in contrast to the surface behaviour of pure carbonyl iron clusters, which, on hydroxylated oxide surfaces, very quickly lose all carbonyls while the iron atoms oxidize [3, 4]. The stabilizing effect of the cyclopentadienyl ligands is quite dramatic.

The present paper deals with analogous studies of the surface reactions of $[(\eta\text{-}C_5H_5)Ru(CO)_2]_2$. Pure ruthenium clusters, like $Ru_3(CO)_{12}$ or bimetallic clusters of the type $Ru_nFe_{3-n}(CO)_{12}$ ($n = 1$–2) do not completely decompose as easily as $Fe_3(CO)_{12}$ even on hydroxylated oxides: on hydroxylated alumina the surface reactions lead to the rather stable anchored surface ruthenium dicarbonyls of the type $Ru^{(0,II,III)}(CO)_2$ [4], while on hydroxylated silica, beside the above dicarbonyl-type end-products, a whole series of molecular ruthenium cluster intermediates occurs [5, 6]. On the other hand, ruthenium cluster frameworks are less favorable for CO ligands in bridging positions. CO-bridged $[(\eta\text{-}C_5H_5)Ru(CO)_2]_2$ in solutions at room temperature has been found to occur in much lower concentrations than $[(\eta\text{-}C_5H_5)Fe(CO)_2]_2$ [7], and thus ruthenium carbonyl clusters containing only μ-CO carbonyls as in the case of iron ($(\eta\text{-}C_5H_5)_2Fe_2(\mu\text{-}CO)_3$, $[(\eta\text{-}C_5H_5)Fe(\mu\text{-}CO)]_4$) are not known. However, –OH groups of hydroxylic solvents form hydrogen bonds with the oxygen atoms of bridging carbonyls of [(η-

0020-1693/91/$3.50

$C_5H_5)Fe(CO)_2]_2$, and so the proportion of the bridged isomers species in these solvents increases [8]. A driving force for the isomerization is the formation of 1:1 and 1:2 adducts by coordination of aluminium (aluminium alkyl) to the oxygen of the bridging carbonyl groups, which have a considerable Lewis base character [9, 10]. Similar interactions are expected with acidic surface sites of oxide supports.

As already mentioned, on oxide surfaces reactions with acidic hydroxyls leading to the insertion of H^+ into the metal–metal bond could not be excluded, either [1, 2]. Reactions of this type have been detected for $[(\eta\text{-}C_5H_5)Fe(CO)_2]_2$ with anhydrous acids [11]. In order to better model this reaction of surface hydroxyls, we performed some FT-IR measurements of the reactions of both $[(\eta\text{-}C_5H_5)Fe(CO)_2]_2$ and $[(\eta\text{-}C_5H_5)Ru(CO)_2]_2$ with $(CF_3)_3COH$ as proton donor in liquid xenon solutions.

Experimental

Measurements on oxide surfaces

$[(\eta\text{-}C_5H_5)Ru(CO)_2]_2$ prepared by the method given in ref. 12 was deposited from pentane solution to an extent of 1 wt.% on alumina (Degussa, Alon C) and silica (Cabot Corporation, Cab-O-Sil HS5), respectively. Prior to impregnation both supports were partially dehydroxylated (573 K, 16 h).

Two types of experiments were performed.

(i) After impregnation, the supported cluster was dried in vacuum, then wetted with paraffin oil (Nujol Mull) and the IR spectrum of the suspension was recorded between two KBr windows. As described elsewhere [1], the presence of paraffin oil slowed down the surface reactions and, therefore, we were able to get information about the very first steps of cluster–support interaction, and to detect surface intermediates of very short lifetime. Infrared spectra were recorded at room temperature.

(ii) In the second method the supported complexes were dried under vacuum and pressed into wafers (10 mg/cm^2) which were then placed in a heatable vacuum IR cell. Infrared spectra, under vacuum, were recorded at temperatures ranging from 303–723 K.

All IR measurements were performed using a Digilab FTS-20C spectrometer. For all spectra reported a 200-scan data accumulation was carried out at a resolution of 2 cm^{-1}. As references we used spectra of partially dehydroxylated alumina and silica in a Nujol mull or spectra recorded at different temperatures of pure oxide wafers, respectively.

In order to detect smaller spectral changes, difference spectra were also computed, and in some cases numerical integration and spectrum analysis by fitting Gaussians to experimental data were carried out.

Measurements in liquid xenon

The measurements of $[(\eta\text{-}C_5H_5)Ru(CO)_2]_2$ and $[(\eta\text{-}C_5H_5)Fe(CO)_2]_2$ in solutions of liquid xenon were performed using a Bruker IFS/113v spectrometer at a resolution of 2 cm^{-1}, with a cooled 7.5 cm pathway cell, as described before [13, 14].

Results

All spectral frequency data used in assignment of the different surface structures, reference frequencies and all structures (molecules and surface bonded species) considered are collected in Table 1. In the text we will refer to these structures by using their numbers (**I**–**X**) given in the first column of Table 1.

$[(\eta\text{-}C_5H_5)Ru(CO)_2]_2/Al_2O_3$/Nujol system

The spectra of the $[(\eta\text{-}C_5H_5)Ru(CO)_2]_2/Al_2O_3$/ Nujol system, recorded at room temperature at different times after impregnation, are seen in Fig. 1(a), and they represent, as mentioned above, the first steps of surface–cluster interaction. Figure 1(a) also includes a spectrum recorded in n-hexane solution of $[(\eta\text{-}C_5H_5)Ru(CO)_2]_2$; the 'o' and '+' signs indicate the non-bridged (open form, structure **I**) and the bridged isomers (**II**), respectively. In Fig. 1(b) the respective difference spectra are shown. Comparing the spectra of the surface species we find that a remarkable quantity of non-bridged, unperturbed open form molecules (**I**) occur on the surface after impregnation, as indicated by the sharp bands at 1972 and 1942 cm^{-1}. The unperturbed (not surface-bonded, only weakly physisorbed) bridged isomer (**II**) clearly indicated by the sharp band at 1792 cm^{-1} also occurs and its relative concentration in comparison to that of open form is about the same as in solution. The relative intensity of the terminal CO band of the *cis* bridged form around 2008 cm^{-1}, however, is much higher than in solution. Taking into account that not only the peak of the terminal CO band is higher but the band is also considerably broader, we believe it originates from strongly perturbed bridged type molecules bonded to the surface, through oxygen atoms of the bridging carbonyls. Therefore the CO stretching mode of these bridging carbonyls should be shifted to lower frequencies and, in the case of the 1:1 complexes, the symmetric band around 1820 cm^{-1} should also be active [1, 2, 8, 9]. The broad and intense band system between 1760–1740 cm^{-1} confirms the pres-

TABLE 1. Spectral data of $[(\eta\text{-}C_5H_5)Ru(CO)_2]_2$ complexes

Structure[a]	Frequencies (cm^{-1})				Conditions	Reference	Stability (K)	Remarks
I 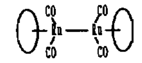	2020	1973	1944		in heptane	ref.7		*cis + trans*
	2024	1976	1946		in liquid xenon	this work		*cis + trans*
		1972	1942		Al_2O_3/Nujol, room T	this work		medium concentration
			1943		SiO_2/Nujol, room T	this work		low concentration
		1970	1945		Al_2O_3/vacuum, T	this work	<353	traces
		1973	1940		SiO_2/vacuum, T	this work	<523	low concentration
II 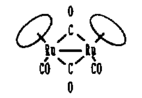	2010	1965		1794	in heptane	ref. 7		*cis + trans*
	2013	1968		1797	in liquid xenon	this work		*cis + trans*
				1792	Al_2O_3/Nujol, room T	this work		low concentration
III 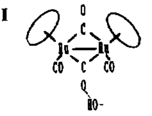		1986	1823	1731	in liquid xenon + $(CF_3)_3COH$	this work		1:1 H-bonded complex
	1997	1963	1808	1754	in methanol	ref. 8		1:1 H-bonded complex
	2008	1963	1818	1740	Al_2O_3/Nujol, room T	this work		medium concentration
	2008	1970	1817	1740	SiO_2/Nujol, room T	this work		low concentration
	2005	1960	1817	1760	Al_2O_3/vacuum, T	this work	<413	low concentration
	2005	1960	1834	1745	Al_2O_3/vacuum, T	this work	<523	high concentration
			1812	1740	SiO_2/vacuum, T	this work	<413	traces
			1834	1740	SiO_2/vacuum, T	this work	<443	traces
IV 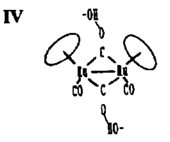	2000	1965		1729	in m/Cresol	ref. 8		1:2 H/bonded complex
		1986		1731	in liquid xenon + $(CF_3)_3COH$	this work		1:2 H-bonded complex
	2008	1963		1740	Al_2O_3/Nujol, room T	this work		medium concentration
	2008	1970		1740	SiO_2/Nujol, room T	this work		high concentration
				1770, 1760	Al_2O_3/vacuum, T	this work	<453	high concentration
	2015	1972		1740–50	SiO_2/vacuum, T	this work	<483	high concentration
				1770	SiO_2/vacuum, T	this work	<443	traces
				1735	SiO_2/vacuum, T	this work	<393	traces
V 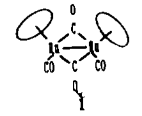	2006	1988	1831	1680	AlR_3	ref. 9		1:1 adducts with Lewis acids
	2020	1975	1846	1675	Al_2O_3/vacuum, T	this work	<483	low concentration
VI 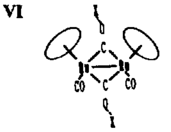	2045	2006		1680	$2AlR_3$	ref. 9		1:2 adducts with Lewis acids
	2035	1990		1695	Al_2O_3/Nujol, room T	this work		medium concentration
				1700	SiO_2/Nujol, room T	this work		low concentration
	2020			1700	SiO_2/vacuum, T	this work	<393	low concentration
VII 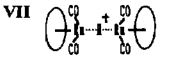	2065	2020			in liquid xenon + $(CF_3)_3COH$	this work		2 rotational
	2071	2026			in liquid xenon + $(CF_3)_3COH$	this work		isomers observed
	2060	2012			Al_2O_3/Nujol, room T	this work		see text
	2062	2015			SiO_2/Nujol, room T	this work		see text
	2062	2015			Al_2O_3/vacuum, T	this work	<443	see text
	2070	2030			SiO_2/vacuum, T	this work	<393	see text
VIII 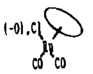	2057	2009			CCl_4, UV	ref. 15		
	2060	2012			Al_2O_3/Nujol, room T	this work		medium concentration
	2062	2015			SiO_2/Nujol, room T	this work		medium concentration
	2062	2015			Al_2O_3/vacuum, T	this work	<443	medium concentration
	2070	2030			SiO_2/vacuum, T	this work	<393	medium concentration
IX $Ru^{II}(CO)_2$	2076	2000			$Ru_3(CO)_{12}/Al_2O_3$	ref. 3	<623	surface anchored species
	2073	2000			Al_2O_3/vacuum, T	this work	<573	medium concentration
X $Ru^{0}(CO)_2$	2062	1989			$Ru_3(CO)_{12}/Al_2O_3$	ref. 3	<623	surface anchored species
	2050	1980			Al_2O_3/vacuum, T	this work	<573	medium concentration

[a] X stands for strong Lewis acid.

ence of a large amount of the 1:2 hydrogen bonded complex with surface hydroxyls (IV), while the less intense band at 1818 cm^{-1} must belong to 1:1 complexes (III) of lower concentration. Considering the very high intensity of the terminal CO band of the bridged *cis* isomer at 2008 cm^{-1}, in contrast to that at 1963 cm^{-1} which belongs to both *cis* and *trans* isomers, we suppose that on the surface mainly *cis* bridged isomers have formed. Adduct type complexes coordinated to strong Lewis acid sites of the surface are also detectable, though in lower concentration only, as indicated by the medium intensity broad band at 1695 cm^{-1}. A pair of weak shoulders at 2035 and 1990 cm^{-1} supposedly also belongs to this 1:2 type adduct (VI).

All spectral frequencies with their assignment are shown in Table 1, along with reference frequencies taken from infrared studies of analogous systems. The experiments in liquid xenon solutions will be discussed later.

In the spectra for the system $[(\eta\text{-}C_5H_5)Ru(CO)_2]_2/Al_2O_3$/Nujol two bands at 2060 and 2012 cm^{-1} (see also the difference spectra in Fig. 2(b)!) slowly increase with time. For this pair of bands two assignments are possible: structure VII protonated form and/or VIII surface bonded monomer. Both possibilities will also be discussed later in connection with the liquid xenon experiments.

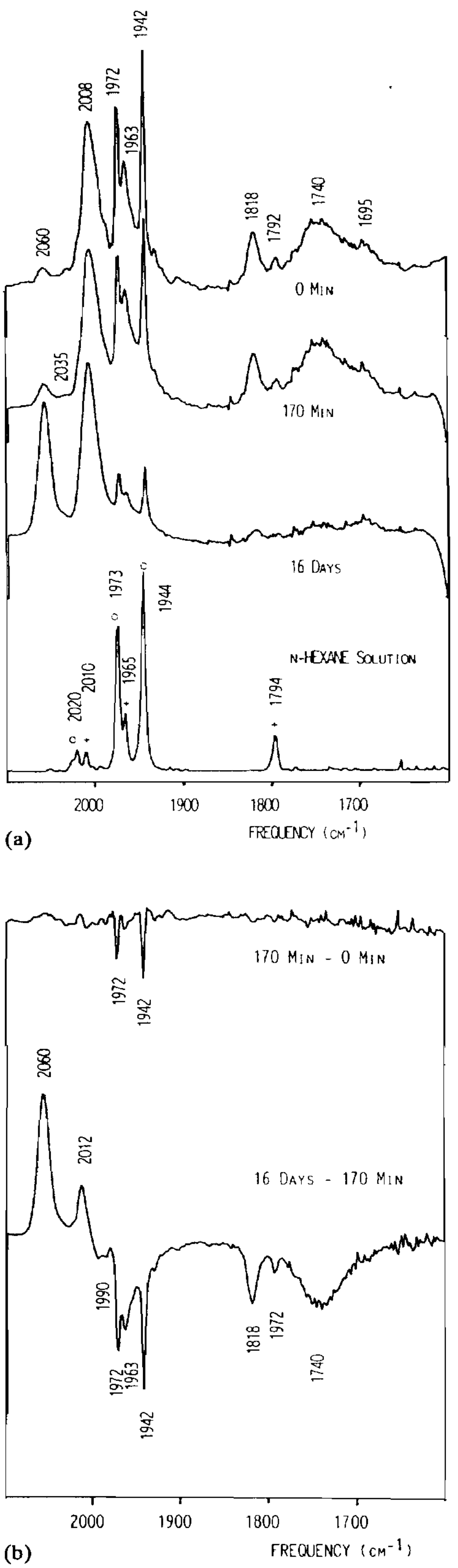

Fig. 1. FT-IR spectra (a) and difference spectra (b) of the $[(\eta\text{-}C_5H_5)Ru(CO)_2]_2/Al_2O_3$/Nujol system.

$[(\eta\text{-}CH_5)Ru(CO)_2]_2/SiO_2$/Nujol system

On silica (Fig. 2(a) and (b)), during the initial steps of surface–cluster interaction we find only slightly different results. The unperturbed open form of the $[(\eta\text{-}C_5H_5)Ru(CO)_2]_2$ molecules is only seen in traces (see the very weak band at 1943 cm^{-1}). No unperturbed bridged molecules have been detected (no band around 1790 cm^{-1}). Most of the molecules are in the *cis* bridged form and they are mostly bonded to the surface by hydrogen bonds of the 1:2 type (because the band indicating 1:1 complexes is very weak). Relatively quickly a pair of bands develops at 2062 and 2015 cm^{-1}, which belongs to the protonated molecule (VII) or to the surface bonded monomer dicarbonyl (VIII). A 1:2 adduct (VI) is indicated by the strongly perturbed band of the bridging carbonyls at 1700 cm^{-1}.

The very low intensity band at 1625 cm^{-1} should also be assigned to bridging carbonyls, which because of the very low frequency should have an unusually high basicity. It is not excluded, either, that a tetramer as in the case of iron in $[(\eta\text{-}C_5H_5)Fe(\mu\text{-}CO)]_4$, might be stabilized on the surface. This possibility, however, does not seem to be confirmed by the present knowledge about ruthenium clusters with bridging carbonyls.

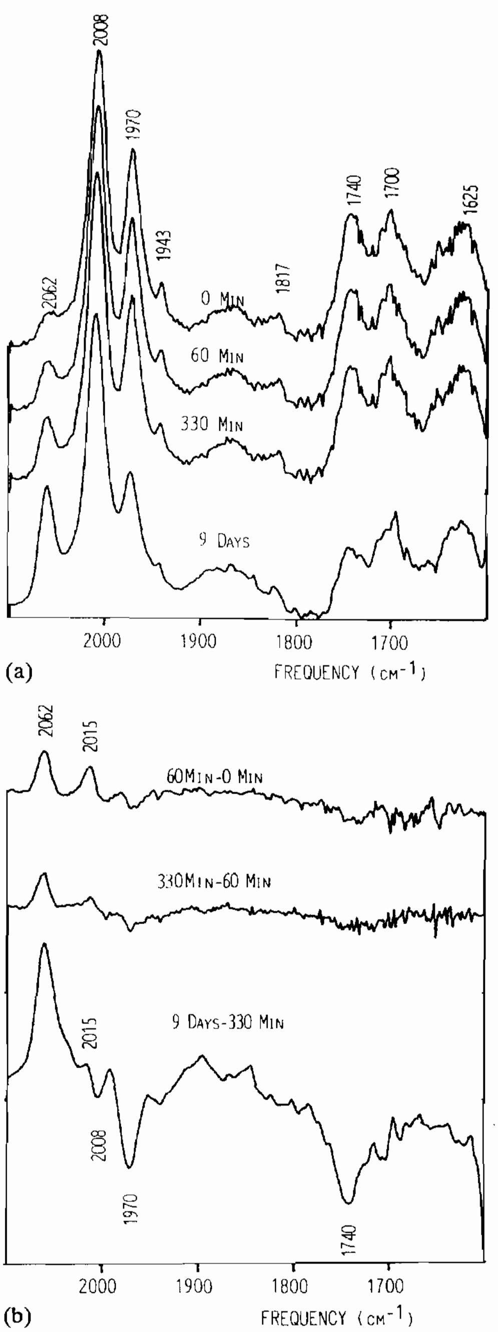

Fig. 2. FT-IR spectra (a) and difference spectra (b) of the $[(\eta\text{-}C_5H_5)Ru(CO)_2]_2/SiO_2$/Nujol system.

$[(\eta\text{-}C_5H_5Ru(CO)_2]_2/Al_2O_3$/vacuum, T system

In this and in the next part we examine the thermal behaviour of the surface species developed on the oxide surfaces.

On hydroxylated alumina, as seen in Fig. 3(a), the spectra are dominated by the strong triad of bands at 2005, 1960 (terminal stretchings) and 1740–60 (asymmetrical bridging CO stretching) cm^{-1}, which apparently is to be assigned to hydrogen bonded complexes of both 1:1 (III) and 1:2 (IV) types. The medium intensity band around 1810–1850 cm^{-1} (symmetrical CO stretching) indicates that the 1:1 hydrogen bonded complex (III) also occurs (in medium concentration). Both bands of the bridging carbonyls, however, are quite complex; they contain several components, each of them representing more or less differing structures. In order to separate the different components, we performed a band analysis by fitting Gaussians to the experimental data between 1850–1800 cm^{-1}. Unfortunately, our attempt to analyse in the same way the complex band between 1800–1700 cm^{-1} failed. We also performed numerical integration in the range of terminal CO stretching modes (2100–1860 cm^{-1}), and in the regions of 1860–1800 and 1800–1700 cm^{-1}. For the band at 1675 cm^{-1} we estimated the intensity data by an approximative (non-iterative) simple fitting procedure. The results are collected in Table 2.

As seen in Table 2, the 1846 cm^{-1} component of the symmetrical stretching modes of bridging carbonyls clearly parallels the asymmetrical stretching at 1675 cm^{-1}. So, this pair of bands both increase with temperature up to 443 K and then disappear between 443 and 483 K. They are assigned to the 1:1 adduct (V). The stretching frequencies of the terminal carbonyls of this adduct can be located in the difference spectra (Fig. 3(b)) at 2020 and 1975 cm^{-1}.

The other two components at 1834 and 1817 cm^{-1} must have their pairs in the complex band system between 1800–1700 cm^{-1} and, as already mentioned, they could not be resolved. They belong to a minimum of two somewhat differing 1:1 hydrogen bonded complexes (III), both complexes first increasing then decreasing with temperature. The integrated intensities of the asymmetric bands between 1800–1700 cm^{-1} do not follow this type of temperature dependence: they monotonically decrease, which means this band system contains not only the bands of the 1:1 complexes, but those belonging to 1:2 hydrogen bonded complex(es) (IV), as well. The first two difference spectra in Fig. 3(b) give some additional information about the nature of structure IV: the negative doublet with 1770 and 1760 cm^{-1} frequencies can be assigned to a complex of type IV, bonded to the surface hydroxyls with very weak hydrogen bondings: the frequency of 1770 cm^{-1} is very close to that of unperturbed molecules (1780–1800 cm^{-1}).

The origin of the band at 1630 cm^{-1}, which quickly decreases with temperature, is not clear. It might belong to a complex containing bridging carbonyls only, as already suggested for the SiO_2/Nujol system.

The medium intensity pair of bands at 2062 and c. 2015 cm^{-1} (the last band overlapping with the

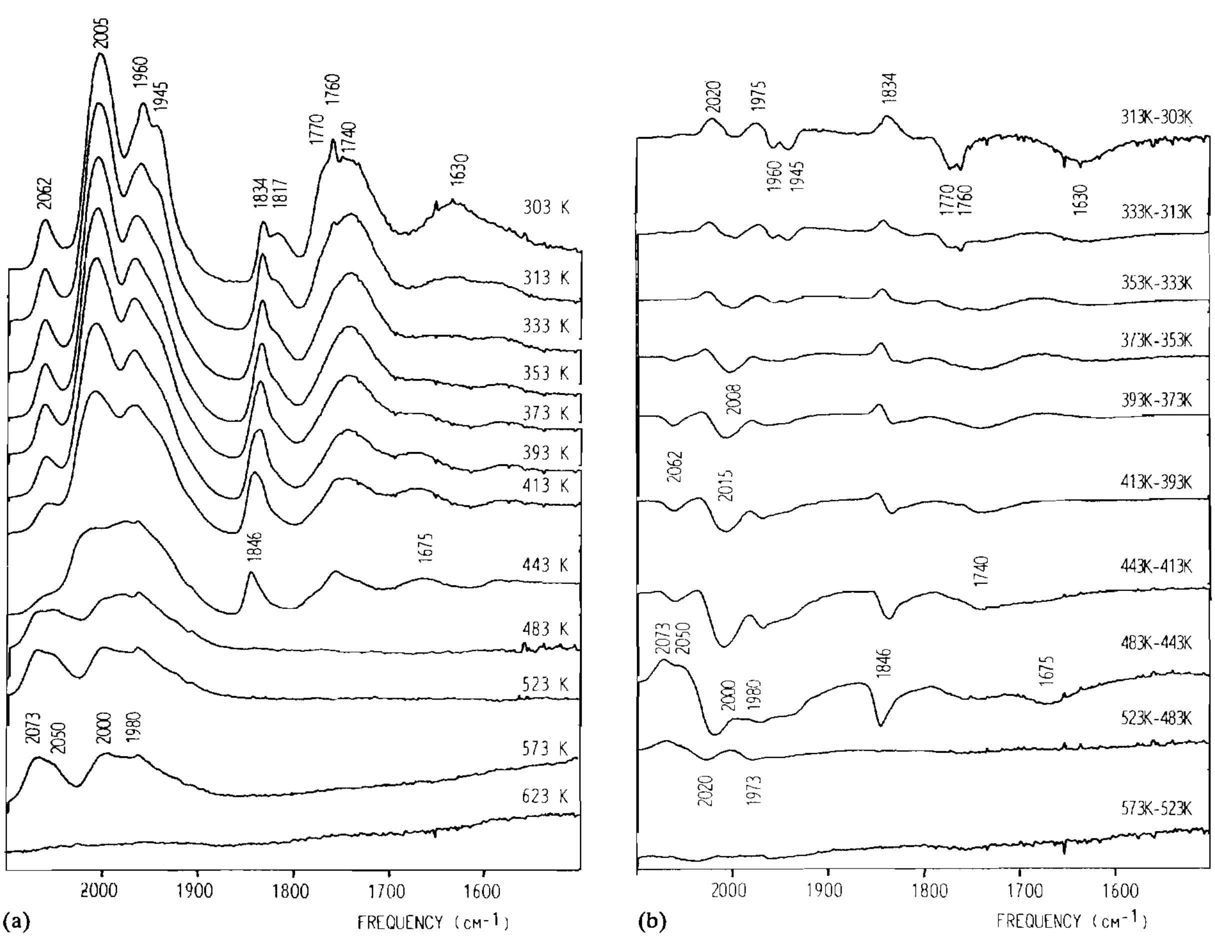

Fig. 3. FT-IR spectra (a) and difference spectra (b) of the $[(\eta\text{-}C_5H_5)Ru(CO)_2]_2/Al_2O_3$ system during thermal treatment in vacuum.

TABLE 2. Intensity data (in arbitrary units) calculated from the spectra of Fig. 3(a) by numerical integration[a] or by curve fitting procedure[b]

Spectrum (K)	Frequency range[a] or band center frequency[b] (cm^{-1})							
	2100–1860[a]	1846[b]	1834[b]	1817[b]	1860–1800[a]	1800–1700[a]	1675[b]	1630[b]
303	6158	≈0	215	231	456	1997	≈0	760
313	6345	≈0	333	204	532	1730		220
333	6371	24	285	277	575	1479	31	40
353	6452	44	300	240	586	1241		≈0
373	6256	84	321	162	590	928	109	
393	5792	101	291	153	542	921		
413		140	233	112	485		201	
443	3728	160	113	220	283	402	298	
483	2436	≈0	≈0	≈0	≈0	320	≈0	

strong band of structure III at 2005 cm^{-1}) should be assigned to the carbonyls of structures VII and VIII (for detailed discussion see the part dealing with the liquid xenon experiments), which disappear in the temperature range of 373–443 K (see difference spectra in Fig. 3(b)).

In the temperature range of 443–583 K new bands at 2073, 2050, 2000 and c. 1980 cm^{-1} develop, which are stable up to 573 K (Fig. 3(a) and (b)). These four bands are well known from studies dealing with the interaction of $Ru_3(CO)_{12}$ and hydroxylated oxide supports: the bands around 2073 and 2000 cm^{-1}

belong to $Ru^{II}(CO)_2$ (IX), while those around 2050 and 1980 cm^{-1} belong to $Ru^0(CO)_2$ (X) surface dicarbonyls both strongly anchored to the surface [3, 4, 16]. The formation of these types of surface carbonyls is always preceded by the cleavage of metal–metal bonds [3, 4] and, in the present case, it should also be preceded by the loss of the cyclopentadienyl ligand.

[(η-C_5H_5)Ru(CO)$_2$]$_2$/SiO$_2$/vacuum, T system

At first sight the spectra in Fig. 4(a) seem to be less complex than those of the system of Al_2O_3/vacuum, T (Fig. 3(a)). Certainly, the dominant surface species on silica support is the 1:2 hydrogen bonded complex (IV) in accordance with the very strong bands at 2015, 1973 (shoulder) and 1740 cm^{-1}. It decomposes between 413–523 K (see the respective difference spectra in Fig. 4(b)).

Structures VII or VIII also occur in medium concentration producing the CO stretching frequencies at 2070 and 2030 cm^{-1}. The lower frequency band can be separated by the difference spectra of the temperature range 333–413 K (from second to sixth difference spectra in Fig. 4(b)). Notice that these frequencies are somewhat higher than the respective frequencies recorded in the case of the alumina support.

One of the most pronounced differences between the surface species occurring on silica and alumina is that on silica 1:1 complexes are only detectable in very low concentrations (see the spectral region of 1850–1800 cm^{-1}). On the other hand, like on alumina, on silica a minimum of two different 1:1 complex structures can be separated according to the two maxima at 1840 and 1812 cm^{-1}.

The band system between 1800–1700 cm^{-1} also contains several components. The main, most intense component, belonging to the 1:2 hydrogen bonded complex (IV) is that at 1740–50 cm^{-1}, which, together with the terminal CO bands at 2015 and 1972 cm^{-1}, are clearly seen on the spectrum recorded at 483 K in Fig. 4(a) and on the difference spectra 483–343 and 523–483 K in Fig. 4(b). On silica the most stable surface species is structure IV; it decomposes between

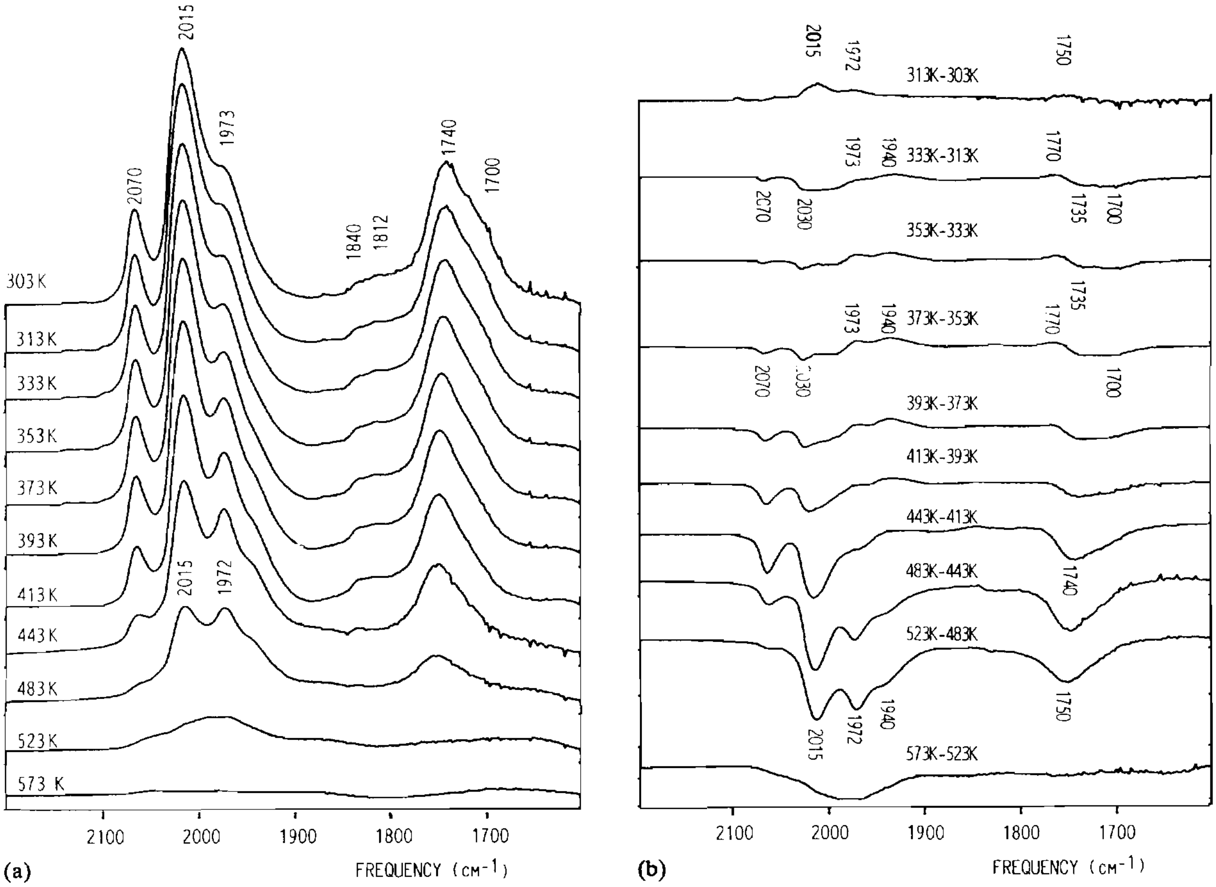

Fig. 4. FT-IR spectra (a) and difference spectra (b) of the [(η-C_5H_5)Ru(CO)$_2$]$_2$/SiO$_2$ system during thermal treatment in vacuum.

443–523 K. Further components (shoulders of low intensities in Fig. 4(a) and more pronounced features in fig. 4(b)) at 1770 and 1735 cm^{-1} indicate the presence of further more or less differing hydrogen bonded structures. The band at 1770 cm^{-1}, which increases with temperature up to *c.* 393 K, apparently belongs to a very weakly bonded complex. The very weak spectral feature at 1700 cm^{-1} just as in the Nujol experiment should be assigned to the 1:2 adduct type complex (VI).

In contrast to alumina, on silica, as seen in the difference spectra of Fig. 4(b), the non-bridged form (I) of $[(\eta\text{-}C_5H_5)Ru(CO)_2]_2$ is relatively stable and, what is more, it is formed by heating the sample (see the positive weak bands in the difference spectra at 1973 and 1940 cm^{-1}) up to *c.* 413 K, and decomposes between 443–523 K.

Another, more essential difference, is that on silica support no $Ru^{0,II}(CO)_2$ anchored species occur. Finally, no band at 1630 cm^{-1} was found (Fig. 4(a)). However, if a sample of the type $[(\eta\text{-}C_5H_5)Ru(CO)_2]_2/SiO_2$/vacuum is kept at room temperature for several days, the above band slowly develops as seen in Fig. 5.

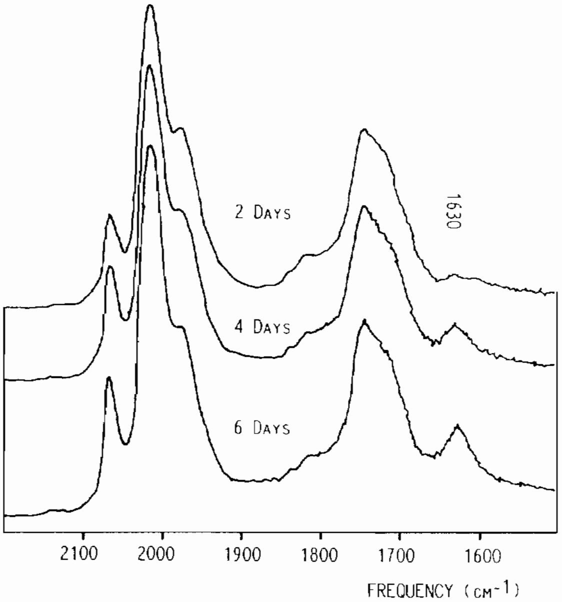

Fig. 5. FT-IR spectra of the $[(\eta\text{-}C_5H_5)Ru(CO)_2]_2/SiO_2$ system kept in vacuum at room temperature.

Reactions of $[(\eta\text{-}C_5H_5)Fe(CO)_2]_2$ and $[(\eta\text{-}C_5H_5)Ru(CO)_2]_2$ in liquid xenon solutions

In Fig. 6 the spectra of $[(\eta\text{-}C_5H_5)Ru(CO)_2]_2+(CF_3)_3COH$ (a) and that of $[(\eta\text{-}C_5H_5)Fe(CO)_2]_2+(CF_3)_3COH$ (b) are recorded for liquid xenon solutions at 165 and 200 K. Spectra A′ and B′ are the respective spectra of the pure compounds in liquid xenon at 200 K.

Detailed studies of the above systems, together with those of further ones, will be published elsewhere. In the present paper we only want to pay attention to the formation of protonated molecules (structure VIII). In the case of the iron complex, the bands of the CO stretching modes assigned to protonated molecule have been detected at 2069 and 2028 cm^{-1} (low temperature form) and at 2064 and 2024 cm^{-1} (high temperature form). For the ruthenium protonated molecule two pairs of bands were also detected; one pair at 2071 and 2026 cm^{-1}, and the other at 2065 and 2020, due to two rotational isomers. The isomer assigned to the higher frequencies is only stable at lower temperatures, while that assigned to the lower frequencies is a high temperature form.

The relative intensities of the bands of the protonated molecules are quite different when comparing the iron complex with that of ruthenium: in the case of iron a very small part, while for ruthenium most of the molecules, are in the protonated form. Further, in both cases we have found that the concentration of the protonated molecules practically did not decrease at high temperature. We notice that in the case of the ruthenium complex, even at 230 K (not shown), the bands which dominate the spectrum, are those belonging to the protonated molecule. This significantly major ability of ruthenium to form $Ru\text{–}H^+\text{–}Ru$ bonds can be explained by the higher basicity of Ru.

Taking into account the above facts, we are convinced that the insertion of a proton into the metal–metal bond, as an initial step leading to the cleavage of this bond, must be a rather probable way for the cluster–support interaction, first of all in the case of the ruthenium complex. Furthermore, in the case of the ruthenium complex, the results of the model experiments in liquid xenon solution suggest that the protonated structure $(\eta\text{-}C_5H_5)(CO)_2Ru\text{–}H^+\text{–}Ru(CO)_2(\eta\text{-}C_5H_5)$, coordinated with the proton to surface O^- anions may also occur.

Discussion

In the case of $[(\eta\text{-}C_5H_5)Fe(CO)_2]_2$, surface reactions with oxide supports produced two main surface species: the $[(\eta\text{-}C_5H_5)(CO)_2Fe\text{–}O\text{–}]$ monomer of medium thermal stability and the $[(\eta\text{-}C_5H_5)Fe(\eta\text{-}CO)]_4$ tetramer of extremely high thermal stability [2].

$[(\eta\text{-}C_5H_5)Ru(CO)_2]_2$, which is in general less reactive than $[(\eta\text{-}C_5H_5)Fe(CO)_2]_2$, seems to better

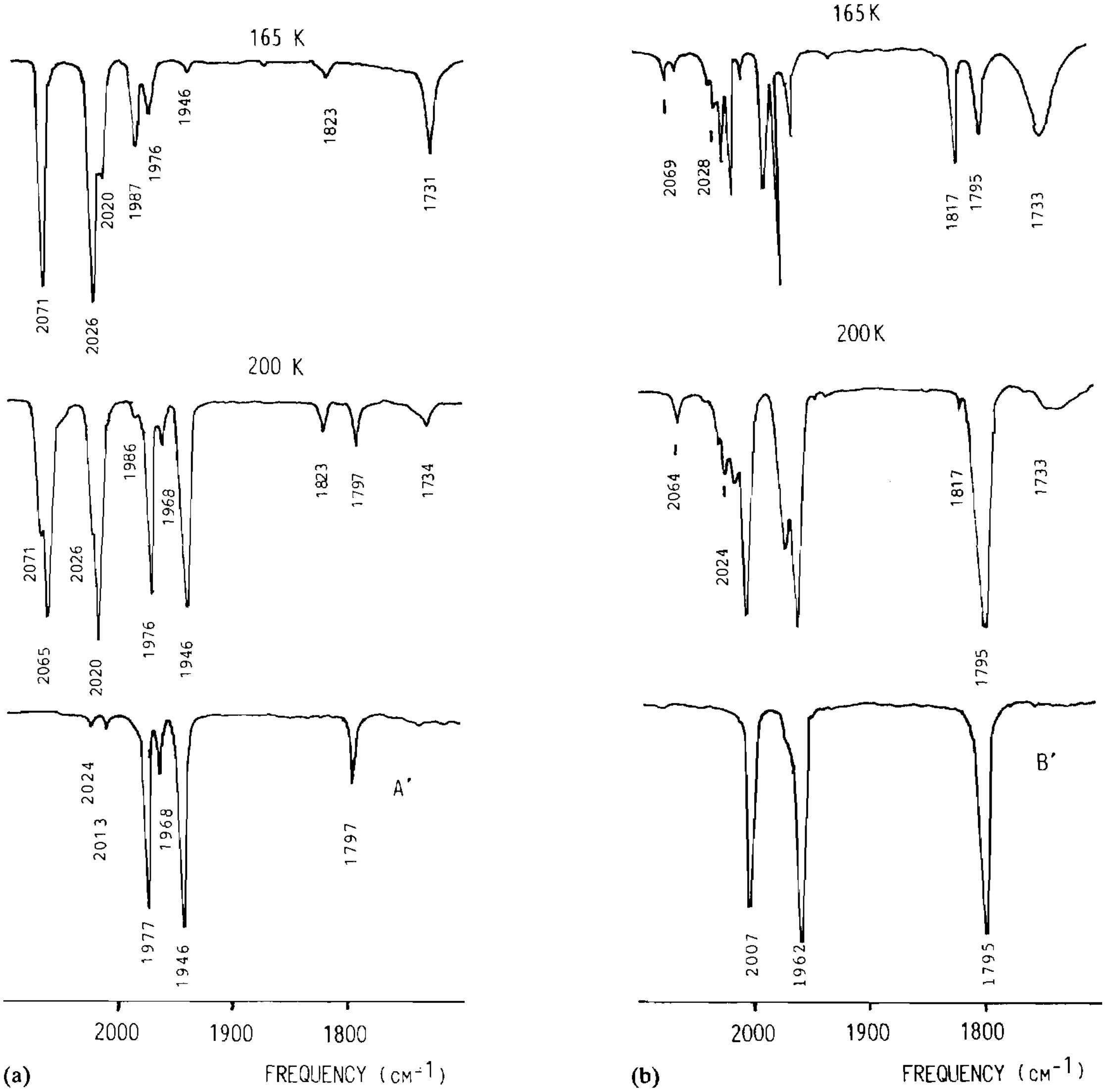

Fig. 6. FT-IR transmission spectra of $[(\eta\text{-}C_5H_5)Ru(CO)_2]_2$ + $(CF_3)_3COH$ (a) and $[(\eta\text{-}C_5H_5)Fe(CO)_2]_2$+$(CF_3)_3COH$ (b) at 165 and 200 K. Spectra A' and B' were recorded in the liquid xenon solution of pure $[(\eta\text{-}C_5H_5)Ru(CO)_2]_2$ and $[(\eta\text{-}C_5H_5)Fe(CO)_2]_2$, respectively.

preserve the entity of the molecule on partially hydroxylated (the hydroxylization of the surface is not complete, both Bronsted and Lewis acid sites are expected, however, Lewis acid sites are in lower concentration) oxide supports.

The main surface species are different types of hydrogen bonded complexes formed between the oxygen atoms of μ-CO groups of $[(\eta\text{-}C_5H_5)Ru(CO)_2]_2$ and the hydrogen of the surface hydroxyls. These complexes are stable up to relatively high temperatures: >443 K on alumina and >523 K on silica. On alumina both 1:1 and 1:2 type hydrogen bonded complexes occur, while on silica mainly those of the 1:2 type occur, the 1:1 type is found only in low concentration.

Adduct type complexes with Lewis acidic sites only occur in low concentration, in accordance with the lower concentration of Lewis acid sites on the surface. As in the case of hydrogen bonded complexes, for alumina 1:1 type adducts are characteristic while for silica they are 1:2 type adducts.

Monomeric cyclopentadienylruthenium anchored to the surface through oxygen atoms ($[(\eta\text{-}C_5H_5)(CO)_2Ru\text{–}O\text{–}]$) is also characteristic for both alumina and silica supported systems. The initial step leading to this surface species is the insertion of a proton donated by Bronsted acid sites into the metal–metal bond forming the (η-C_5H_5)-$(CO)_2$Ru–H^+–Ru$(CO)_2$(η-C_5H_5) molecule. This intermediate molecule, however, may be also stabilized by coordination to O^- ions of the surface, and in this way it can coexist on the surface with the [(η-C_5H_5)$(CO)_2$Ru–O–] monomer, which forms in the second step of this reaction.

IR spectroscopy, unfortunately, cannot distinguish between (η-C_5H_5)$(CO)_2$Ru–H^+–Ru$(CO)_2$(η-C_5H_5) and [(η-C_5H_5)$(CO)_2$Ru–O–] surface species. However, model experiments performed in liquid xenon solutions using $(CF_3)_3COH$ as acid, suggest that the protonated molecule is stable up to relatively high temperatures. The ability of [(η-C_5H_5)Ru$(CO)_2$]$_2$ to form a protonated molecule is considerably higher than that of [(η-C_5H_5)Fe$(CO)_2$]$_2$. This fact suggests that insertion of a proton into the metal–metal bond can also happen to the open form [(η-C_5H_5)Ru$(CO)_2$]$_2$, taking into account that the concentration of open form in solutions of [(η-C_5H_5)Ru$(CO)_2$]$_2$ in comparison to that of [(η-C_5H_5)Fe$(CO)_2$]$_2$ is much higher. The mechanism suggested by Manning starts from the bridged form [(η-C_5H_5)M$(CO)_2$]$_2$ being attacked by an electrophile that can be H^+ [17]. If we consider that stable salts of protonated [(η-C_5H_5)Ru$(CO)_2$]$_2$ are also known, all facts seem to support our opinion that protonated molecules can also occur on the surface. On the other hand, the existence of [(η-C_5H_5)$(CO)_2$Ru–O–] on the surface should not be excluded, either, because it can also form not only from (η-C_5H_5)$(CO)_2$Ru–H^+–Ru$(CO)_2$(η-C_5H_5), but, under the experimental conditions we used, by a photochemically induced symmetrical cleavage of [(η-C_5H_5)Ru$(CO)_2$]$_2$, where the (η-C_5H_5)Ru$(CO)_2$) radical fragments could be stabilized by surface oxygens.

It should be mentioned that an unsymmetrical cleavage of (η-C_5H_5)$(CO)_2$Ru–H^+–Ru$(CO)_2$(η-C_5H_5) to [(η-C_5H_5)Ru$(CO)_3$]$^+$ is not excluded, either, as we found for [(η-C_5H_5)Fe$(CO)_2$]$_2$ adsorbed on silica [2]. In fact, its absence in all systems of the present work is rather surprising, although the presence of coordinating anion, like surface O^-, is very favorable to a cleavage to [(η-C_5H_5)$(CO)_2$Ru–O–]. Although we have not detected any [(η-C_5H_5)Ru$(CO)_3$]$^+$ in this work, its formation as a short-lifetime intermediate should be supposed.

Just as in liquid xenon solutions, a reversibility between open form [(η-C_5H_5)Ru$(CO)_2$]$_2$, CO bridged [(η-C_5H_5)Ru$(CO)_2$]$_2$, hydrogen bonded (or adduct) [(η-C_5H_5)Ru$(CO)_2$]$_2$ and protonated [(η-C_5H_5)Ru$(CO)_2$]$_2$ should be supposed on the surface, too. (Such a reversibility cannot be valid for surface species already anchored to the surface, like [(η-C_5H_5)$(CO)_2$Ru–O–] and/or any surface species produced by decomposition of [(η-C_5H_5)Ru$(CO)_2$]$_2$.) The reversibility is supported by the presence of all the above molecules on the surface, and first of all by the fact experienced on silica surface, where with increasing temperature the concentration of open form [(η-C_5H_5)Ru$(CO)_2$]$_2$ increases.

The appearance of $Ru^0(CO)_2$ and $Ru^{II}(CO)_2$ surface anchored species on alumina at higher temperatures must be due to reactions which may have rather complex mechanisms. Thermal and photochemically induced reactions in solutions leading to the break down of the metal–ring bonding are known for both iron and ruthenium cyclopentadienylcarbonyls [18, 19]. These reactions start from the salts of the [(η-C_5H_5)M$(CO)_3$]$^+$ (M = Fe, Ru) cation, which is a possible product of the unsymmetrical cleavage of the (η-C_5H_5)$(CO)_2$M–H^+–M$(CO)_2$(η-C_5H_5) molecule. Although we have not detected the formation of [(η-C_5H_5)Ru$(CO)_3$]$^+$, its occurrence as a short-lifetime intermediate, as mentioned above, is very probable. In our opinion, however, the very high thermal stability of both $Ru^0(CO)_2$ and $Ru^{II}(CO)_2$ surface anchored species might play a very important role by involving mechanism(s) differing from those known in solution.

In the case of [(η-C_5H_5)Fe$(CO)_2$]$_2$, the most interesting surface species was the only μ-CO containing, extremely stable [(η-C_5H_5)Fe(μ-CO)]$_4$ tetramer. Such a stable surface molecule has not been detected in the case of [(η-C_5H_5)Ru$(CO)_2$]$_2$. It should be mentioned that a band found around 1630 cm^{-1} might indicate the occurrence of a molecule containing only bridging carbonyls. This molecule is of low thermal stability. Our attempt to assign it failed.

References

1 S. Dobos, S. Nunziante-Cesaro and B. V. Lokshin, *J. Mol. Struct.*, *174* (1988) 325.

2 S. Dobos and A. Beck, *Inorg. Chim. Acta*, *176* (1990) 163.

3 S. Dobos, I. Boszormenyi, J. Mink and L. Guczi, *Inorg. Chim. Acta*, *120* (1986) 135.

4 S. Dobos, I. Boszormenyi, J. Mink and L. Guczi, *Inorg. Chim. Acta*, *120* (1986) 145.

5 S. Dobos, I. Boszormenyi, J. Mink and L. Guczi, *Inorg. Chim. Acta*, *134* (1987) 203.

6 S. Dobos, I. Boszormenyi, J. Mink and L. Guczi, *Inorg. Chim. Acta*, *144* (1988) 37.

7 P. McArdle and A. R. Manning, *J. Chem. Soc. A*, (1970) 2128.

8 P. McArdle and A. R. Manning, *J. Chem. Soc. A*, (1970) 2133.

9 A. Alich, N. J. Nelson and D. F. Shriver, *Chem. Commun.*, (1971) 254.

10 A. Alich, N. J. Nelson, D. Strope and D. F. Shriver, *Inorg. Chem.*, *11* (1972) 2976.

11 D. A. Symon and T. C. Waddington, *J. Chem. Soc. A*, (1971) 953.

12 A. P. Humphries and S. A. P. Knox, *J. Chem. Soc., Dalton Trans.*, (1975) 1710.

13 B. V. Lokshin, S. G. Kazarian and A. G. Ginzburg, *J. Mol. Struct.*, *174* (1988) 29.

14 Ya. M. Kimelfeld, *Russ. Chem. Rev.*, *57* (1988) 730.

15 H. B. Abrahamson, M. C. Palazzotto, C. L. Reichel and M. S. Wrighton, *J. Am. Chem. Soc.*, *101* (1979) 4123.

16 (a) A. Zecchina, E. Guglielminotti, A. Bossi and M. Camia, *J. Catal.*, *74* (1982) 225; (b) E. Guglielminotti, A. Zecchina, A. Bossi and A. Camia, *J. Catal.*, *74* (1982) 240; (c) A. Zecchina, A. Bossi and A. Camia, *J. Catal.*, *74* (1982) 252.

17 A. R. Manning, *Coord. Chem. Rev.*, *51* (1983) 41.

18 T. H. Whitesides and J. Shelly, *J. Organomet. Chem.*, *92* (1975) 215.

19 A. P. Humphries and S. A. R. Knox, *Chem. Commun.*, (1973) 327.